

Supporting Information for

Pairing nanoarchitectonics of oligodeoxyribonucleotides with complex diversity: concatemers and self-limited complexes

Anastasia A. Zamoskvtseva, Victor M. Golyshev, Valeria A. Kizilova, Georgiy Yu Shevelev, Dmitrii V. Pyshnyi and Alexander A. Lomzov*

Anastasia A. Zamoskvtseva^{1,2†}, Victor M. Golyshev^{1†}, Valeria A. Kizilova^{1‡}, Georgiy Yu.

Shevelev¹, Dmitrii V. Pyshnyi¹ and Alexander A. Lomzov^{1}*

¹ Institute of Chemical Biology and Fundamental Medicine, SB RAS, 8 Lavrentiev Avenue, Novosibirsk 630090. Russia

² Moscow Institute of Physics and Technology, 9 Institutskiy per., Dolgoprudny, 141701, Russia

*Corresponding author:
lomzov@niboch.nsc.ru

Table of Contents

| | |
|---|------------|
| Theoretical analysis | S3 |
| Gel shift assay analysis | S6 |
| Thermal denaturation analysis | S10 |
| Atomic force microscopy | S12 |
| Molecular dynamics simulation and analysis | S15 |

Theoretical analysis

In accordance with the thermodynamic scheme in Figure 2, the emergence of a bimolecular self-limited complex in the presence of the **S** component can be described by the following equations:

$$[MN^{11}] = K_2 \cdot [M] \cdot [N]$$

$$[MN^{22}] = K_1 \cdot [M] \cdot [N]$$

$$[MN^*] = K_1 \cdot K_{h2} \cdot [M] \cdot [N]$$

(1)

$$[NS] = K_s \cdot [N] \cdot [S]$$

$$[MNS] = K \cdot K_s \cdot [M] \cdot [N] \cdot [S]$$

where $K_{1,2,h1,h2,s,s2} = \exp(-\Delta G^0_{1,2,h1,h2,s,s2}(T)/R/T) = \exp(-(\Delta H^0_{1,2,h1,h2,s,s2} - T \cdot \Delta S^0_{1,2,h1,h2,s,s2})/R/T)$ are equilibrium constants of the formation of intermolecular complexes by fragment 1, 2, or **s**, whereas K_{h1} or K_{h2} are equilibrium constants of intramolecular complex formation (T : temperature, K ; R : gas constant, $1.987 \text{ cal}\cdot\text{K}^{-1}\cdot\text{mol}^{-1}$). In combination with mass balance equations (2) for oligonucleotides **M**, **N**, and **S**, the above formulas give a system of algebraic equations

$$[M]_0 = [MN^{11}] + [MN^{22}] + [NS] + [MNS] + [MN^*] + [M]$$

$$[N]_0 = [MN^{11}] + [MN^{22}] + [MNS] + [MN^*] + [N]$$

(2)

$$[S]_0 = [NS] + [MNS] + [S].$$

For simplicity's sake, in the theoretical analysis, thermal stability levels of blocks 1 and 2 were assumed to be the same ($K_1 = K_2 = K$ and therefore $K_{h1} = K_{h2} = K_h$), and equimolar total concentrations of **M** and **N** were postulated ($[M]_0 = [N]_0$). This approach significantly decreases the complexity of the analysis, similarly to the analysis for a concatemer complex that we described in our previous papers [22,37]. We used a numerical solver for the system of equations (1, 2) to determine **M**, **N**, and **S** at given concentrations ($[M]_0 = [N]_0$, $[S]_0$), thermodynamic parameters ($\Delta H^0_{1,2,h,s}$ and $\Delta S^0_{1,2,h,s}$), and temperature (T).

For a given $[M]_0$ the equilibrium among all oligonucleotides' forms can be shifted to one side or another if $[S]_0$, K_s , or both are changed. K_s values can be varied by means of the temperature or by changing the length and/or nucleotide composition of the **s** block or buffering conditions (by changing ΔH^0 and ΔS^0). By adjusting these two parameters, we can open a bimolecular self-limited complex. Examination of the redistribution of components' concentrations in solution (using, for example, gel electrophoresis) under the influence of changes in the binding constant (i.e., temperature) or in the **S** component concentration will help to prove the formation of bimolecular V-shaped complexes or complexes higher molecularity. The latter ploy is easily implemented at a constant temperature. A suitable range of changes in **S** concentration—for the detection by gel electrophoresis—is a 10-fold deficiency to a 10-fold excess relative to $[M]_0$.

In the presence of linear and circular tetramolecular (or higher-order) complexes, the

thermodynamic analysis was hampered considerably. The algebraic equations for determining the concentrations will have a higher degree and a very narrow convergence region. Therefore, the system of equations cannot be solved numerically by relatively simple methods. Nonetheless, the proposed approach of S component concentration variation can help determine molecularity values of self-limited complexes. Gradual addition of S to self-limited tetramolecular complex $\mathbf{M}_2\mathbf{N}_2^*$ (Figure 1d) yields linear penta- ($\mathbf{M}_2\mathbf{N}_2\mathbf{S}$) (Figure 1m) and trimolecular (\mathbf{MNS}) (Figure 1l) complexes. The detection of such components during a stepwise increase of “opener” concentration is a way to determine the molecularity of the complex.

Typical melting curves calculated as changes in concentration of all single-stranded blocks during a temperature increase for non-lengthened S oligomers and those lengthened by 4 nt are shown in Figure S1.

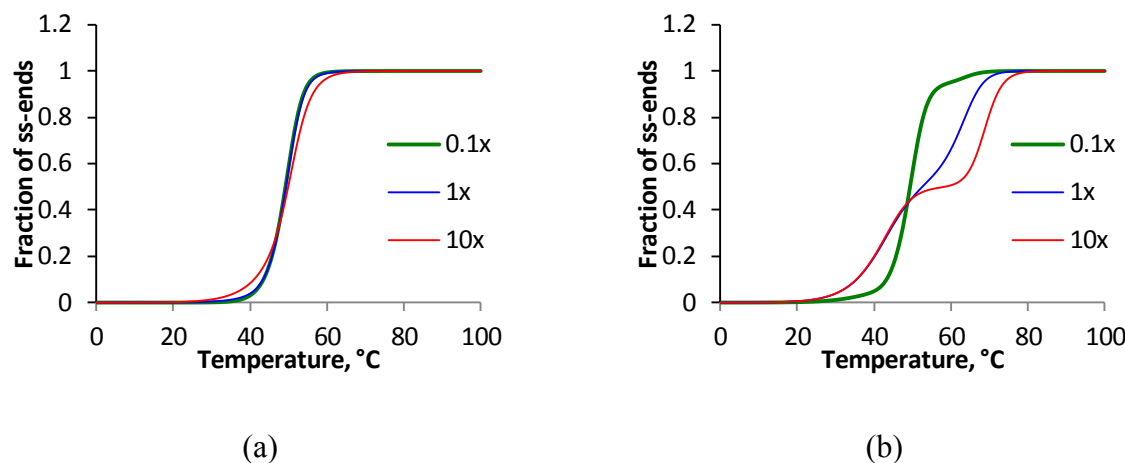


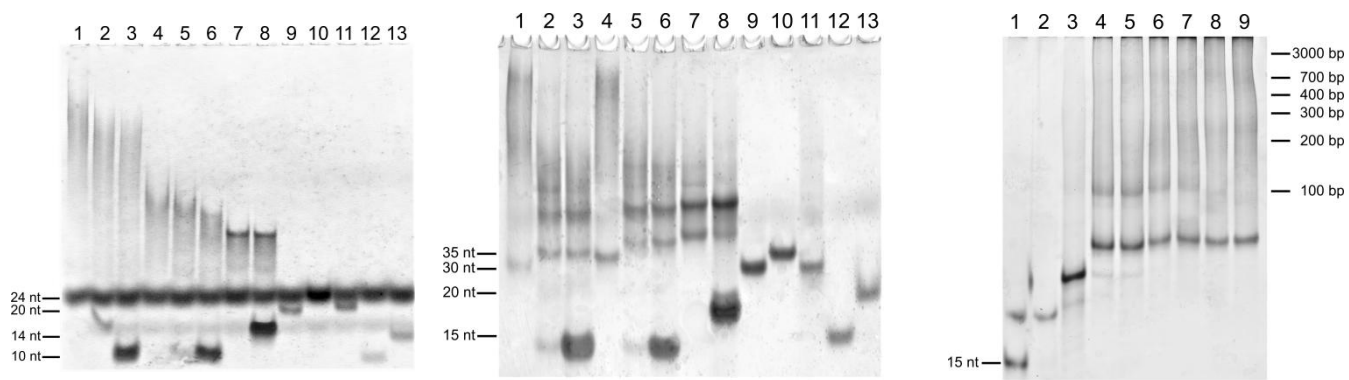
Figure S1. Calculated thermal denaturation curves for the proposed thermodynamic scheme at different S concentrations: (a) non-lengthened complex M20D/N20D in the presence of S10; (b) M20D/N20Dl complex of oligomers with a lengthened s block in the presence of S10l.

Table S1. Thermodynamic parameters used in theoretical analysis of M20/N20 complex

| Sequence 5'->3' | ΔH^0. cal/mol | ΔS^0. cal/mol/K | T_m, °C |
|---------------------------|---|---|--------------------------|
| CTAACTAACG | -69255 | -195 | 42.1 |
| CCATCATATG | -69473 | -197 | 41.5 |
| CTAACTAACGCGAC | -104401 | -287 | 62.4 |
| CTAACTAACGCGA | -93711 | -257 | 59.5 |
| CTAACTAACGCG | -87179 | -240 | 56.8 |
| CTAACTAACGC | -79279 | -221 | 49.9 |

Additional penalty for intramolecular complex formation (K_h) was taken -14 cal/mol/K of only entropic contribution.

Gel shift assay analysis



(a) **(b)** **(c)**
Figure S2. The gel shift assay of oligonucleotides' complexes of various lengths without linkers.
(a) Lanes: 1, M20/N20 (1:1); 2, M20/N20/S10 (1:1:1); 3, M20/N20/S10 (1:1:10); 4, M20/N20l (1:1); 5, M20/N20l/S10 (1:1:1); 6, M20/N20l/S10 (1:1:10); 7, M20/N20l/S10l (1:1:1); 8, M20/N20l/S10l (1:1:10); 9, N20; 10. N20l; 11, M20; 12, S10; 13, S10l.
(b) Lanes: 1, M30/N30 (1:1); 2, M30/N30/S15 (1:1:1); 3, M30/N30/S15 (1:1:10); 4, M30l/N30 (1:1); 5, M30l/N30/S15 (1:1:1); 6, M30l/N30/S15 (1:1:10); 7, M30l/N30/S15l (1:1:1); 8, M30l/N30/S15l (1:1:10); 9, M30; 10. M30l; 11, N30; 12, S15; 13, S15l.
(c) Lanes: 1, ladder; 2, M40/SX15 (2:1); 3, M40/SX15 (1:1); 4, M40/S15/S25 (1:1:1); 5, M40/N40/SX15 (1:1:10); 6, M40/N40/SX15 (1:1:5); 7, M40/N40/SX15 (1:1:1); 8, M40/N40/SX15 (1:1:0.5); 9, M40/N40/SX15 (1:1:0.1); 10. M40/N40 (1:1) (experiment at 15 °C).

| (a) | | (b) | | (c) | |
|------|------------------------|------|------------------------|------|------------------------|
| Line | Sample | Line | Sample | Line | Sample |
| 1 | M20/N20 (1:1) | 1 | M30/N30 | 1 | ladder |
| 2 | M20/N20/S10 (1:1:1) | 2 | M30/N30/S15 (1:1:1) | 2 | M40/SX15 (2:1) |
| 3 | M20/N20/S10 (1:1:10) | 3 | M30/N30/S15 (1:1:10) | 3 | M40/SX15 (1:1) |
| 4 | M20/N20I (1:1) | 4 | M30I/N30 (1:1) | 4 | M40/S15/S25 (1:1:1) |
| 5 | M20/N20I/S10 (1:1:1) | 5 | M30I/N30/S15 (1:1:1) | 5 | M40/N40/SX15 (1:1:10) |
| 6 | M20/N20I/S10 (1:1:10) | 6 | M30I/N30/S15 (1:1:10) | 6 | M40/N40/SX15 (1:1:5) |
| 7 | M20/N20I/S10I (1:1:1) | 7 | M30I/N30/S15I (1:1:1) | 7 | M40/N40/SX15 (1:1:1) |
| 8 | M20/N20I/S10I (1:1:10) | 8 | M30I/N30/S15I (1:1:10) | 8 | M40/N40/SX15 (1:1:0.5) |
| 9 | N20 | 9 | M30 | 9 | M40/N40/SX15 (1:1:0.1) |
| 10 | N20I | 10 | M30I | 10 | M40/N40 (1:1) |
| 11 | M20 | 11 | N30 | | |
| 12 | S10 | 12 | S15 | | |
| 13 | S10I | 13 | S15I | | |

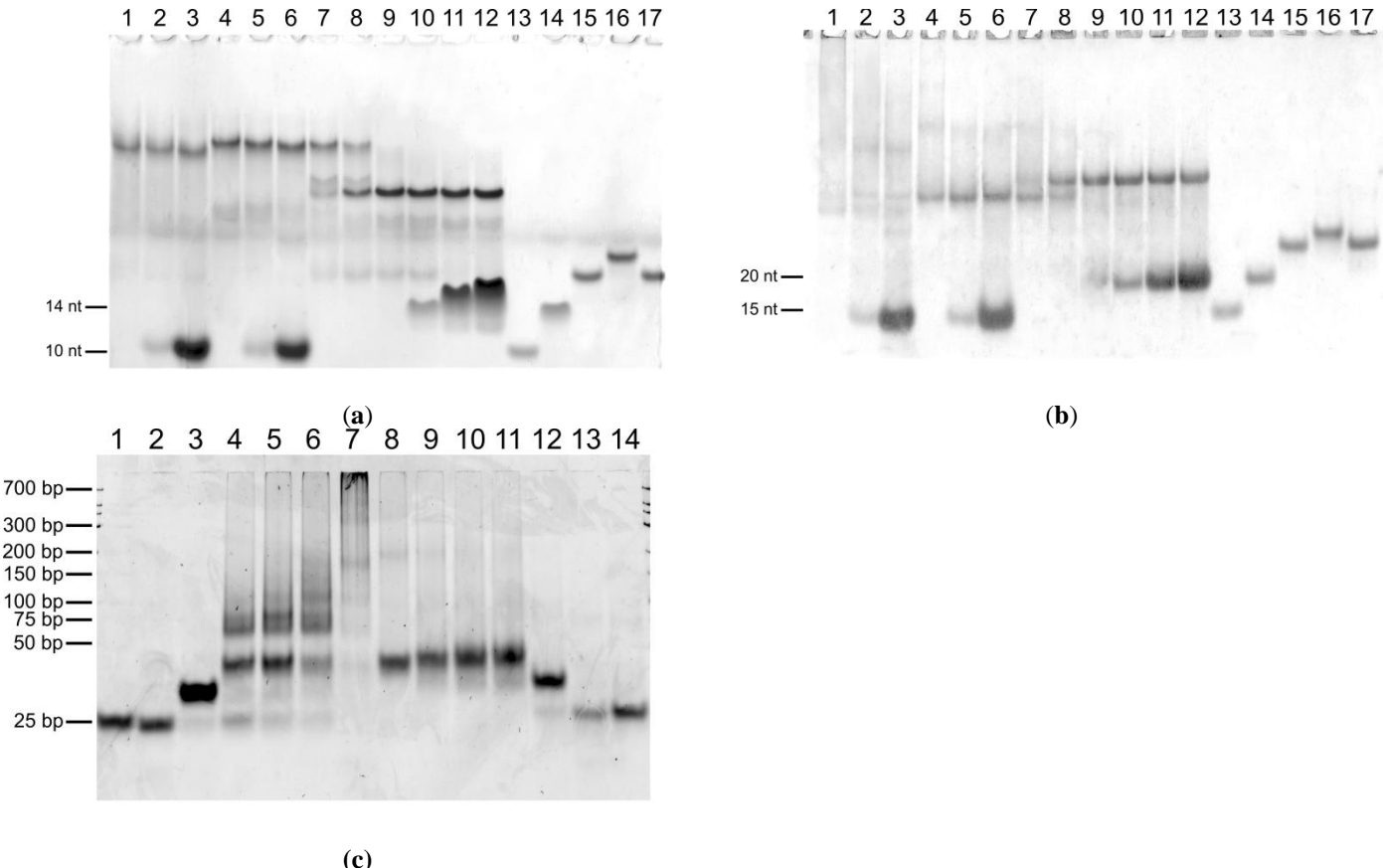


Figure S3. Determination of complex molarity. Gel shift assay of oligonucleotides' complexes of various lengths carrying non-nucleotide linkers and different concentration of the S component: **(a)** Lanes: 1, M20D/N20D (1:1); 2, M20D/N20D/S10 (1:1:1); 3, M20D/N20D/S10 (1:1:10); 4, M20D/N20Dl (1:1); 5, M20D/N20Dl/S10 (1:1:1); 6, M20D/N20Dl/S10 (1:1:10); 7, M20D/N20Dl/S10l (1:1:0.25); 8, M20D/N20Dl/S10l (1:1:0.5); 9, M20D/N20Dl/S10l (1:1:1); 10, M20D/N20Dl/S10l (1:1:2); 11, M20D/N20Dl/S10l (1:1:5); 12, M20D/N20Dl/S10l (1:1:10); 13, S10l; 14, N20D; 15, N20Dl; 16, M20D. **(b)** Lanes: 1, M30/N30 (1:1); 2, M30/N30/S15 (1:1:1); 3, M30/N30/S15 (1:1:10); 4, M30Dl/N30D (1:1); 5, M30Dl/N30D/S15 (1:1:1); 6, M30Dl/N30D/S15 (1:1:10); 7, M30Dl/N30D/S15l (1:1:0.25); 8, M30Dl/N30D/S15l (1:1:0.5); 9, M30Dl/N30D/S15l (1:1:1); 10, M30Dl/N30D/S15l (1:1:2); 11, M30Dl/N30D/S15l (1:1:5); 12, M30Dl/N30D/S15l (1:1:10); 13, S15l; 14, S15l; 15, M30D; 16, M30Dl; 17, N30D. **(c)** Lanes: 1, ladder 25-700 bp. (Fermentas, Latvia); 2, M30/S15 (1:1); 3, M30/S15-2 (1:1); 4, M30/S15/S15-2 (1:1:1); 5, M30/N30/S15 (1:1:10); 6, M30/N30/S15 (1:1:5); 7, M30/N30/S15 (1:1:1); 8, M30/N30 (1:1); 9, M30D/N30D (1:1); 10, M30D/N30D/S15 (1:1:1); 11, M30D/N30D/S15 (1:1:5); 12, M30D/N30D/S15 (1:1:10); 13, M30D/S15/S15-2 (1:1:1); 14, M30D/S15-2 (1:1); 15, M30D/S15 (1:1). 16, ladder 25-700 bp. (Fermentas, Latvia). This gel shift assay was performed under specific conditions: it was run in a 15% polyacrylamide gel in a 39:1 ratio; SYBR Green I 10000X (Invitrogen, USA) was used to stain the gel.

| (a) | | (b) | | (c) | |
|------|----------------------------|------|----------------------------|------|------------------------|
| Line | Sample | Line | Sample | Line | Sample |
| 1 | M20D/N20D (1:1) | 1 | M30/N30 (1:1) | 1 | ladder 25-700 bp |
| 2 | M20D/N20D/S10 (1:1:1) | 2 | M30/N30/S15 (1:1:1) | 2 | M30/S15 (1:1) |
| 3 | M20D/N20D/S10 (1:1:10) | 3 | M30/N30/S15 (1:1:10) | 3 | M30/S15-2 (1:1) |
| 4 | M20D/N20D1 (1:1) | 4 | M30D1/N30D (1:1) | 4 | M30/S15/S15-2 (1:1:1) |
| 5 | M20D/N20D1/S10 (1:1:1) | 5 | M30D1/N30D/S15 (1:1:1) | 5 | M30/N30/S15 (1:1:10) |
| 6 | M20D/N20D1/S10 (1:1:10) | 6 | M30D1/N30D/S15 (1:1:10) | 6 | M30/N30/S15 (1:1:5) |
| 7 | M20D/N20D1/S10I (1:1:0.25) | 7 | M30D1/N30D/S15I (1:1:0.25) | 7 | M30/N30/S15 (1:1:1) |
| 8 | M20D/N20D1/S10I (1:1:0.5) | 8 | M30D1/N30D/S15I (1:1:0.5) | 8 | M30/N30 (1:1) |
| 9 | M20D/N20D1/S10I (1:1:1) | 9 | M30D1/N30D/S15I (1:1:1) | 9 | M30D/N30D (1:1) |
| 10 | M20D/N20D1/S10I (1:1:2) | 10 | M30D1/N30D/S15I (1:1:2) | 10 | M30D/N30D/S15 (1:1:1) |
| 11 | M20D/N20D1/S10I (1:1:5) | 11 | M30D1/N30D/S15I (1:1:5) | 11 | M30D/N30D/S15 (1:1:5) |
| 12 | M20D/N20D1/S10I (1:1:10) | 12 | M30D1/N30D/S15I (1:1:10) | 12 | M30D/N30D/S15 (1:1:10) |
| 13 | S10 | 13 | S15 | 13 | M30D/S15/S15-2 (1:1:1) |
| 14 | S10I | 14 | S15I | 14 | M30D/S15-2 (1:1) |
| 15 | N20D | 15 | M30D | 15 | M30D/S15 (1:1) |
| 16 | N20D1 | 16 | M30D1 | 16 | ladder 25-700 bp |
| 17 | M20D | 17 | N30D | | |

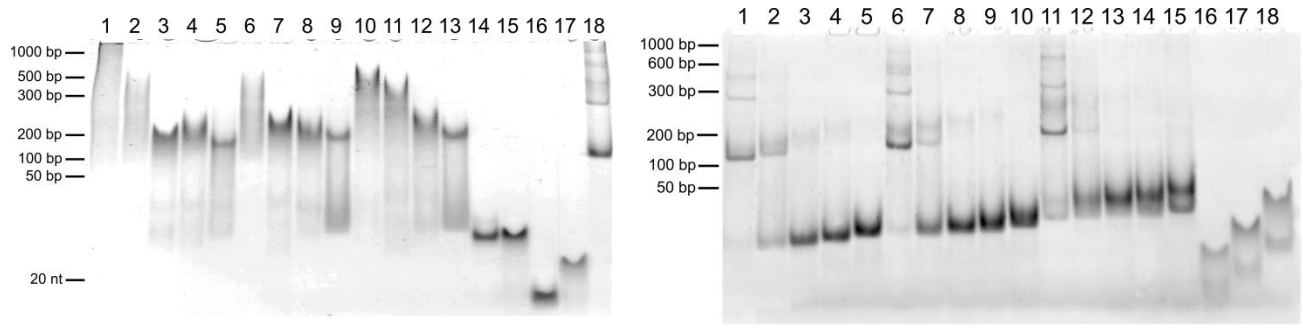


Figure S4. Gel shift assay of oligonucleotide complexes carrying nucleotide linkers of various lengths. **(a)** Lanes: 0. ladder 50-1000 bp (SibEnzyme, Russia); 1, M20/N20; 2, M20T1/N20; 3, M20T2/N20; 4, M20T3/N20; 5, M20T5/N20; 6, M20T1/N20T1; 7, M20T2/N20T1; 8, M20T3/N20T1; 9, M20T5/N20T1; 10, M20T1/N20T2; 11, M20T2/N20T2; 12, M20T3/N20T2; 13, M20T5/N20T2; 14, N20T1; 15, N20T2; 16, M20; 17, N20; 18, M20/N20T3;
(b) Lanes: 0. ladder 50-1000 bp (SibEnzyme, Russia); 1, M20T7/N20; 2, M20T7/N20T1; 3, M20T7/N20T2; 4, M20T7/N20T3; 5, M20T7/N20T5; 6, M20T10/N20; 7, M20T10/N20T1; 8, M20T10/N20T2; 9, M20T10/N20T3; 10, M20T10/N20T5; 11, M20T15/N20; 12, M20T15/N20T1; 13, M20T15/N20T2; 14, M20T15/N20T3; 15, M20T15/N20T5; 16, M20T7; 17, M20T10; 18, M20T15.

| (a) | | (b) | |
|------|-------------|------|--------------|
| Line | Sample | Line | Sample |
| 1 | M20/N20 | 1 | M20T7/N20 |
| 2 | M20T1/N20 | 2 | M20T7/N20T1 |
| 3 | M20T2/N20 | 3 | M20T7/N20T2 |
| 4 | M20T3/N20 | 4 | M20T7/N20T3 |
| 5 | M20T5/N20 | 5 | M20T7/N20T5 |
| 6 | M20T1/N20T1 | 6 | M20T10/N20 |
| 7 | M20T2/N20T1 | 7 | M20T10/N20T1 |
| 8 | M20T3/N20T1 | 8 | M20T10/N20T2 |
| 9 | M20T5/N20T1 | 9 | M20T10/N20T3 |
| 10 | M20T1/N20T2 | 10 | M20T10/N20T5 |
| 11 | M20T2/N20T2 | 11 | M20T15/N20 |
| 12 | M20T3/N20T2 | 12 | M20T15/N20T1 |
| 13 | M20T5/N20T2 | 13 | M20T15/N20T2 |
| 14 | N20T1 | 14 | M20T15/N20T3 |
| 15 | N20T2 | 15 | M20T15/N20T5 |
| 16 | M20 | 16 | M20T7 |
| 17 | N20 | 17 | M20T10 |
| 18 | M20/N20T3 | 18 | M20T15 |

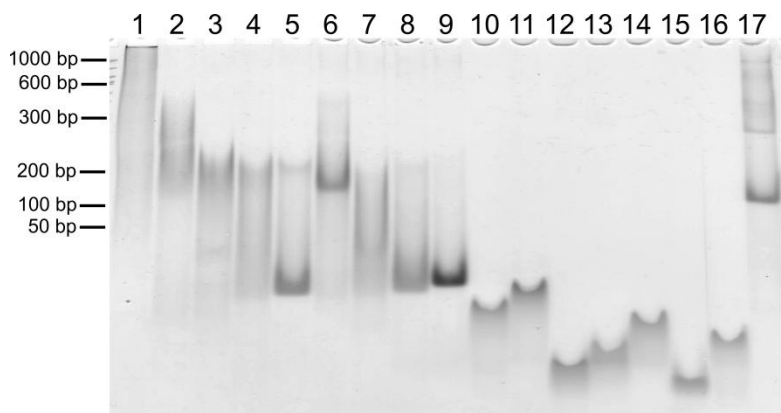
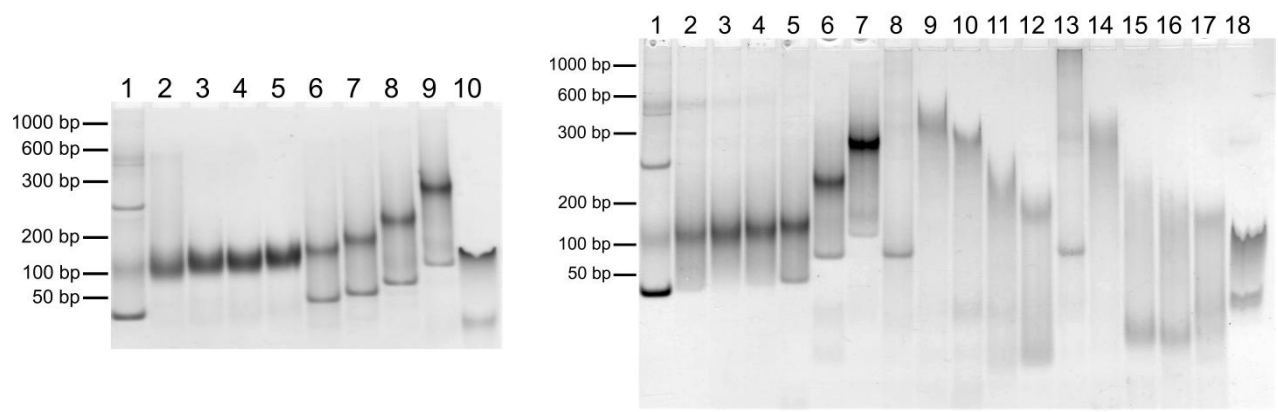


Figure S5. Gel shift assay of oligonucleotides complexes carrying nucleotide linkers of various lengths. Lanes: 0. Ladder 50-1000 bp (SibEnzyme, Russia); 1, M20/N20; 2, M20T1/N20T3; 3, M20T2/N20T3; 4, M20T3/N20T3; 5, M20T5/N20T3; 6, M20T1/N20T5; 7, M20T2/N20T5; 8, M20T3/N20T5; 9, M20T5/N20T5; 10, N20T3; 11, N20T5; 12, M20T2; 13, M20T3; 14, M20T5; 15, M20; 16, N20; 17, M20/N20T3.

| Line | Sample |
|------|-------------|
| 1 | M20/N20 |
| 2 | M20T1/N20T3 |
| 3 | M20T2/N20T3 |
| 4 | M20T3/N20T3 |
| 5 | M20T5/N20T3 |
| 6 | M20T1/N20T5 |
| 7 | M20T2/N20T5 |
| 8 | M20T3/N20T5 |
| 9 | M20T5/N20T5 |
| 10 | N20T3 |
| 11 | N20T5 |
| 12 | M20T2 |
| 13 | M20T3 |
| 14 | M20T5 |
| 15 | M20 |
| 16 | N20 |
| 17 | M20/N20T3 |

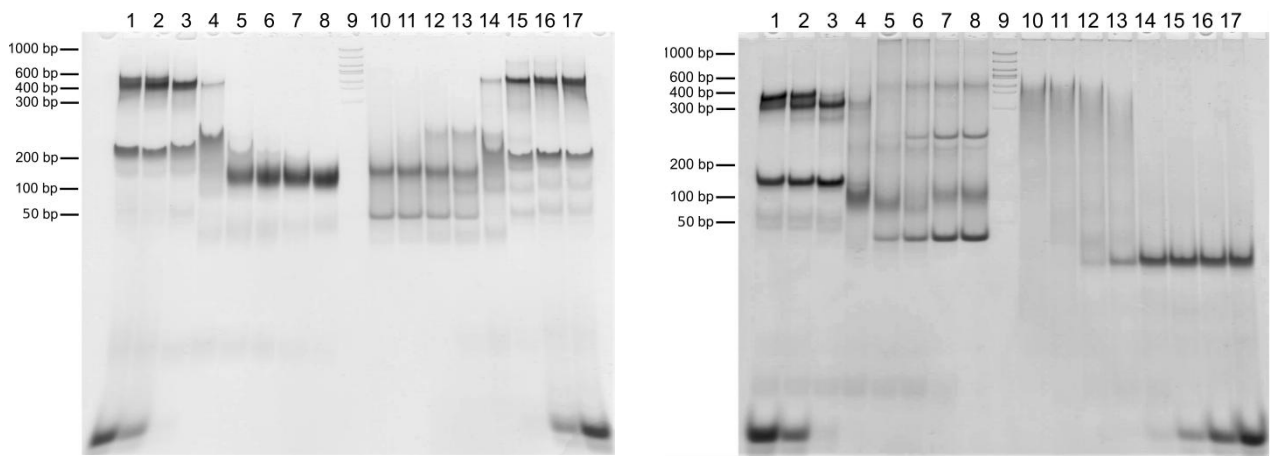


(a)

(b)

Figure S6. Gel shift assay of oligonucleotides complexes carrying nucleotide linkers of various lengths: **(a)** Lanes: 1, M20/N20T25; 2, M20T1/N20T25; 3, M20T2/N20T25; 4, M20T3/N20T25; 5, M20T5/N20T25; 6, M20T7/N20T25; 7, M20T10/N20T25; 8, M20T15/N20T25; 9, M20T25/N20T25; 10, N20T25; **(b)** 1, M20T25/N20; 2, M20T25/N20T1; 3, M20T25/N20T2; 4, M20T25/N20T3; 5, M20T25/N20T5; 6, M20T25/N20T15; 7, M20T25/N20T2; 8, M20/N20T2; 9, M20T1/N20T2; 10, M20T2/N20T2; 11, M20T3/N20T2; 12, M20T5/N20T2; 13, M20/N20T2/S10; 14, M20T1/N20T2/S10; 15, M20T2/N20T2/S10; 16, M20T3/N20T2/S10; 17, M20T5/N20T2/S10; 18, M20T25.

| (a) | | (b) | |
|------|---------------|------|-----------------|
| Line | Sample | Line | Sample |
| 1 | M20/N20T25 | 1 | M20T25/N20 |
| 2 | M20T1/N20T25 | 2 | M20T25/N20T1 |
| 3 | M20T2/N20T25 | 3 | M20T25/N20T2 |
| 4 | M20T3/N20T25 | 4 | M20T25/N20T3 |
| 5 | M20T5/N20T25 | 5 | M20T25/N20T5 |
| 6 | M20T7/N20T25 | 6 | M20T25/N20T15 |
| 7 | M20T10/N20T25 | 7 | M20T25/N20T2 |
| 8 | M20T15/N20T25 | 8 | M20/N20T2 |
| 9 | M20T25/N20T25 | 9 | M20T1/N20T2 |
| 10 | N20T25 | 10 | M20T2/N20T2 |
| | | 11 | M20T3/N20T2 |
| | | 12 | M20T5/N20T2 |
| | | 13 | M20/N20T2/S10 |
| | | 14 | M20T1/N20T2/S10 |
| | | 15 | M20T2/N20T2/S10 |
| | | 16 | M20T3/N20T2/S10 |
| | | 17 | M20T5/N20T2/S10 |
| | | 18 | M20T25 |



(a)

(b)

Figure S7. Gel shift assay of complexes of oligonucleotides with different concentration of S:
(a) Lanes: 1, M20T5/N20T25/S10A5 (1:1:10); 2, M20T5/N20T25/S10A5 (1:1:5); 3, M20T5/N20T25/S10A5 (1:1:2); 4, M20T5/N20T25/S10A5 (1:1:1); 5, M20T5/N20T25/S10A5 (1:1:0.5); 6, M20T5/N20T25/S10A5 (1:1:0.25); 7, M20T5/N20T25/S10A5 (1:1:0.1); 8, M20T5/N20T25; 9, Ladder 50-1000 bp (SibEnzyme, Russia); 10, M20T7/N20T25; 11, M20T7/N20T25/S10A5 (1:1:0.1); 12, M20T7/N20T25/S10A5 (1:1:0.25); 13, M20T7/N20T25/S10A5 (1:1:0.5); 14, M20T7/N20T25/S10A5 (1:1:1); 15, M20T7/N20T25/S10A5 (1:1:2); 16, M20T7/N20T25/S10A5 (1:1:5); 17, M20T7/N20T25/S10A5 (1:1:10); **(b)** 1, M20T1/N20T2/S10A5 (1:1:10); 2, M20T1/N20T2/S10A5 (1:1:5); 3, M20T1/N20T2/S10A5 (1:1:2); 4, M20T1/N20T2/S10A5 (1:1:1); 5, M20T1/N20T2/S10A5 (1:1:0.5); 6, M20T1/N20T2/S10A5 (1:1:0.25); 7, M20T1/N20T2/S10A5 (1:1:0.1); 8, M20T1/N20T2; 9, Ladder 50-1000 bp (SibEnzyme, Russia); 10, M20T1/N20T2; 11, M20T1/N20T2/S10A5 (1:1:0.1); 12, M20T1/N20T2/S10A5 (1:1:0.25); 13, M20T1/N20T2/S10A5 (1:1:0.5); 14, M20T1/N20T2/S10A5 (1:1:1); 15, M20T1/N20T2/S10A5 (1:1:2); 16, M20T1/N20T2/S10A5 (1:1:5); 17, M20T1/N20T2/S10A5 (1:1:10).

| (a) | | (b) | |
|------|-------------------------------|------|-------------------------------|
| Line | Sample | Line | Sample |
| 1 | M20T5/N20T25/S10A5 (1:1:10) | 1 | M20T1/N20T25/S10A5 (1:1:10) |
| 2 | M20T5/N20T25/S10A5 (1:1:5) | 2 | M20T1/N20T25/S10A5 (1:1:5) |
| 3 | M20T5/N20T25/S10A5 (1:1:2) | 3 | M20T1/N20T25/S10A5 (1:1:2) |
| 4 | M20T5/N20T25/S10A5 (1:1:1) | 4 | M20T1/N20T25/S10A5 (1:1:1) |
| 5 | M20T5/N20T25/S10A5 (1:1:0.5) | 5 | M20T1/N20T25/S10A5 (1:1:0.5) |
| 6 | M20T5/N20T25/S10A5 (1:1:0.25) | 6 | M20T1/N20T25/S10A5 (1:1:0.25) |
| 7 | M20T5/N20T25/S10A5 (1:1:0.1) | 7 | M20T1/N20T25/S10A5 (1:1:0.1) |
| 8 | M20T5/N20T25 | 8 | M20T1/N20T25 |
| 9 | Ladder 50-1000 bp | 9 | Ladder 50-1000 bp |
| 10 | M20T7/N20T25 | 10 | M20T1/N20T2 |
| 11 | M20T7/N20T25/S10A5 (1:1:0.1) | 11 | M20T1/N20T2/S10A5 (1:1:0.1) |
| 12 | M20T7/N20T25/S10A5 (1:1:0.25) | 12 | M20T1/N20T2/S10A5 (1:1:0.25) |
| 13 | M20T7/N20T25/S10A5 (1:1:0.5) | 13 | M20T1/N20T2/S10A5 (1:1:0.5) |
| 14 | M20T7/N20T25/S10A5 (1:1:1) | 14 | M20T1/N20T2/S10A5 (1:1:1) |
| 15 | M20T7/N20T25/S10A5 (1:1:2) | 15 | M20T1/N20T2/S10A5 (1:1:2) |
| 16 | M20T7/N20T25/S10A5 (1:1:5) | 16 | M20T1/N20T2/S10A5 (1:1:5) |
| 17 | M20T7/N20T25/S10A5 (1:1:10) | 17 | M20T1/N20T2/S10A5 (1:1:10) |

Thermal denaturation analysis

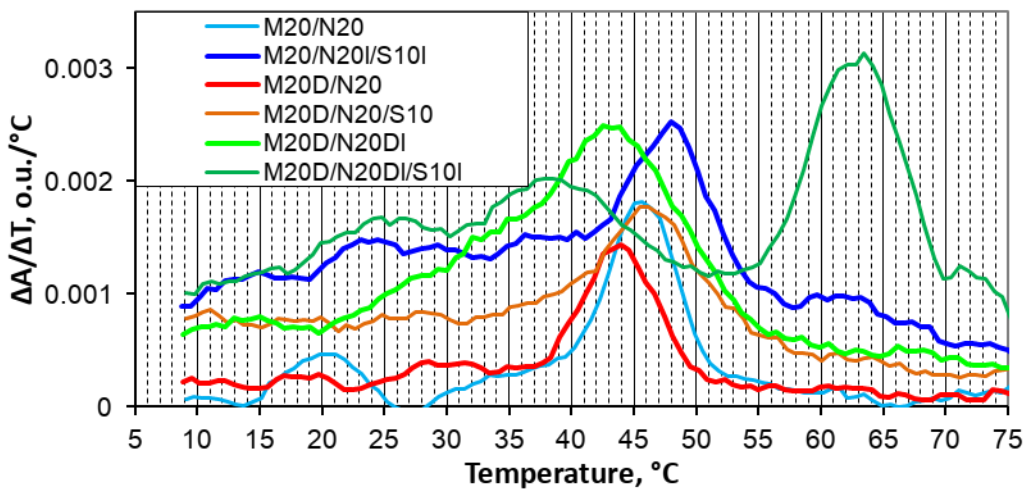


Figure S8. Differential UV melting temperatures of “20-series” complexes without S-component and at 10-fold excess.

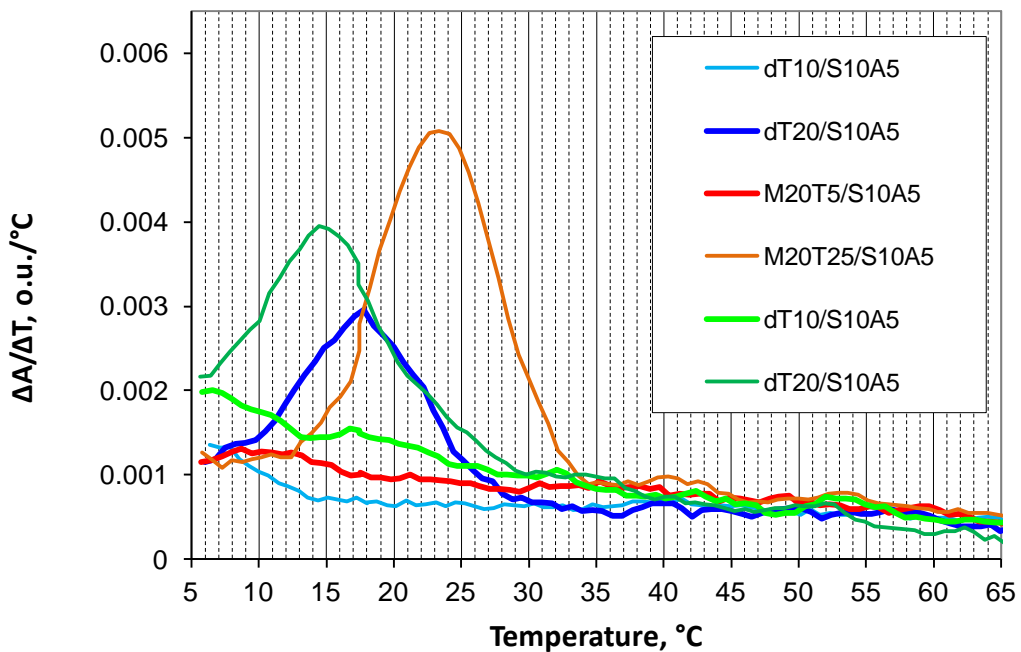


Figure S9. Differential UV melting temperatures of S10A5 complexes with particularly complement oligonucleotides.

Table S2. Melting temperatures of studied complexes with 10 nt duplex blocks. The number in the columns of the oligonucleotides indicates the concentration of the oligomer in solution $\times 10^{-5}$ M.

| | M20 | N20 | M20D | N20D | N20DI | S10 | S10I | T °C |
|----|-----|-----|------|------|-------|-----|------|-------|
| 1 | 1 | 1 | | | | | | 48.6 |
| 2 | 1 | 1 | | | | 10 | | 49.5 |
| 3 | 1 | 1 | | | | | 10 | 50 |
| 4 | | 1 | 1 | | | | | 45.7 |
| 5 | | 1 | 1 | | | | 10 | 47 |
| 6 | | 1 | 1 | | | | 10 | 47 |
| 7 | 1 | | | 1 | | | | 44 |
| 8 | 1 | | | 1 | | 10 | | 44 |
| 9 | 1 | | | 1 | | | 10 | 44 |
| 10 | 1 | | | | 1 | | | 46 |
| 11 | 1 | | | | 1 | 10 | | 46 |
| 12 | 1 | | | | 1 | | 10 | 64/41 |
| 13 | | | 1 | | 1 | | | 40 |
| 14 | | | 1 | | 1 | 10 | | 44 |
| 15 | | | 1 | | 1 | | 10 | 64/39 |
| 16 | | | 1 | 1 | | | | 42 |
| 17 | | | 1 | 1 | | 10 | | 42.5 |
| 18 | | | 1 | 1 | | | 10 | 42.5 |
| 19 | | 1 | | | | 10 | | 47 |
| 20 | | | | 1 | | 10 | | 45 |
| 21 | | | | | 1 | 10 | | 46 |
| 22 | | 1 | | | | | 10 | 47 |
| 23 | | | | 1 | | | 10 | 44 |
| 24 | | | | | 1 | | 10 | 64 |

Table S3. Melting temperatures of studied complexes with 15 nt duplex blocks. The number in the columns of the oligonucleotides indicates the concentration of the oligomer in solution $\times 10^{-5}$ M.

| | M30 | N30 | M30D | N30D | M30DI | S15 | S15I | T °C |
|-----|-----|-----|------|------|-------|-----|------|------|
| 1. | 1 | 1 | | | | | | 58 |
| 2. | 1 | 1 | | | | 10 | | 59 |
| 3. | 1 | 1 | | | | | 10 | 60 |
| 4. | | 1 | 1 | | | | | 58 |
| 5. | | 1 | 1 | | | 10 | | 59 |
| 6. | | 1 | 1 | | | | 10 | 60 |
| 7. | | 1 | | | 1 | | | 62 |
| 8. | | 1 | | | 1 | 10 | | 59 |
| 9. | | 1 | | | 1 | | 10 | 68 |
| 10. | 1 | | | 1 | | | | 59 |
| 11. | 1 | | | 1 | | | | 61 |
| 12. | 1 | | | 1 | | | | 61 |
| 13. | | | 1 | 1 | | | | 59 |
| 14. | | | 1 | 1 | | | | 60 |
| 15. | | | 1 | 1 | | | | 61 |
| 16. | | | 1 | 1 | 1 | | | 62 |
| 17. | | | 1 | 1 | 1 | | | 62 |
| 18. | | | 1 | 1 | 1 | | | 68 |
| 19. | 1 | | | | | 10 | | 55 |
| 20. | | | | 1 | | 10 | | 57 |
| 21. | | | | | 1 | 10 | | 56 |
| 22. | 1 | | | | | | 10 | 57 |
| 23. | | | | 1 | | | 10 | 54 |
| 24. | | | | | 1 | | 10 | 68 |

Atomic force microscopy

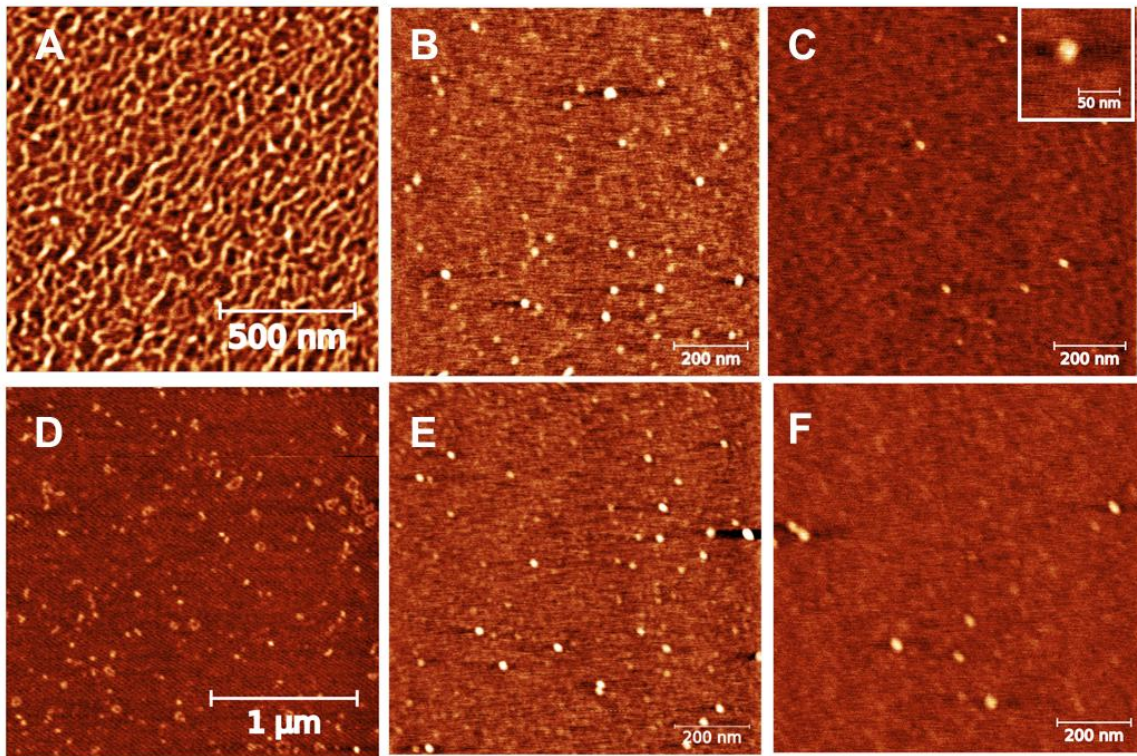


Figure S10. Typical AFM images of the studied complexes: concatemer complex M20/N20 with 90 seconds (A) and 15 seconds (D) exposition, self-limited complex M20D/N20D1 with 45 seconds (B) and 30 seconds (E) exposition, trimolecular complex M20D/N20D1/S10l (C and F).

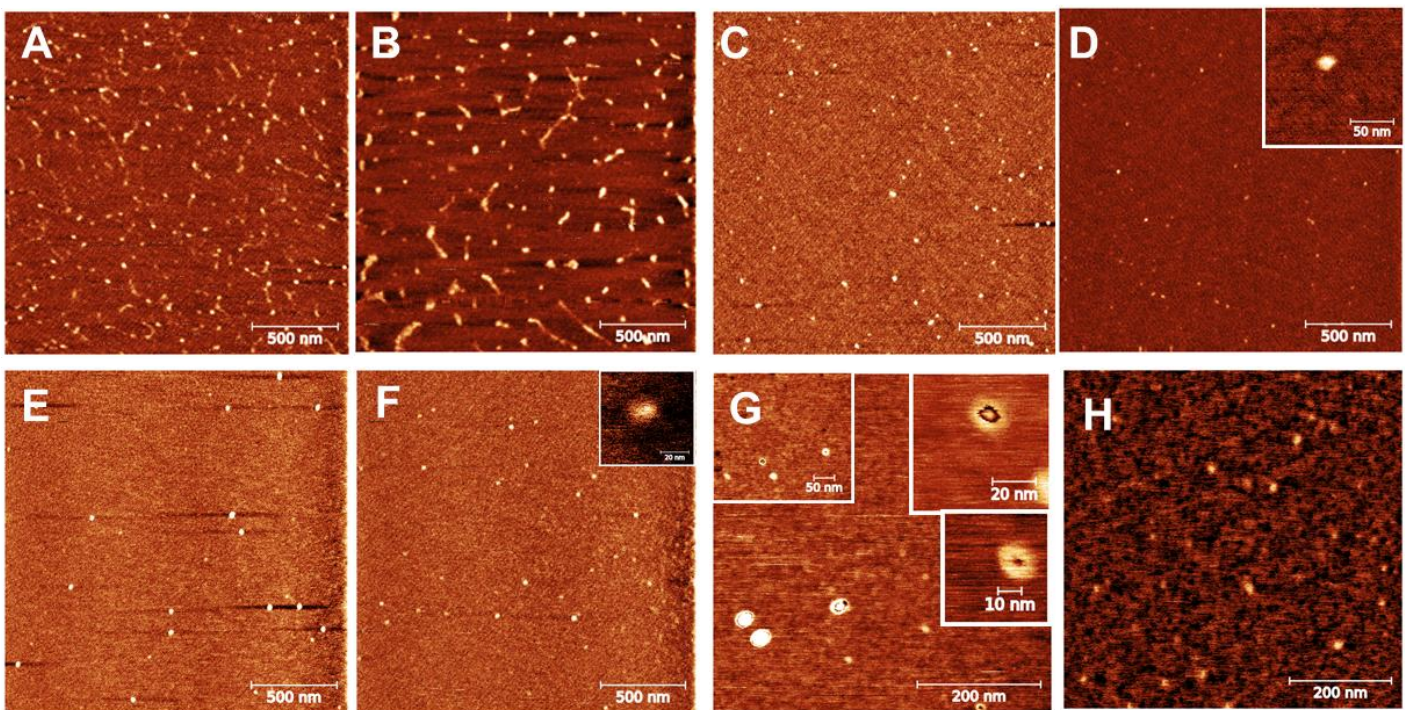


Figure S11. Typical AFM images of the studied complexes: M20T1/N20 (A, B), M20/N20T3 (C, D), M20T5/N20T5 (E), M20T5/N20 (F), M20T1/N20T2(G), M20/N20T25 (H).

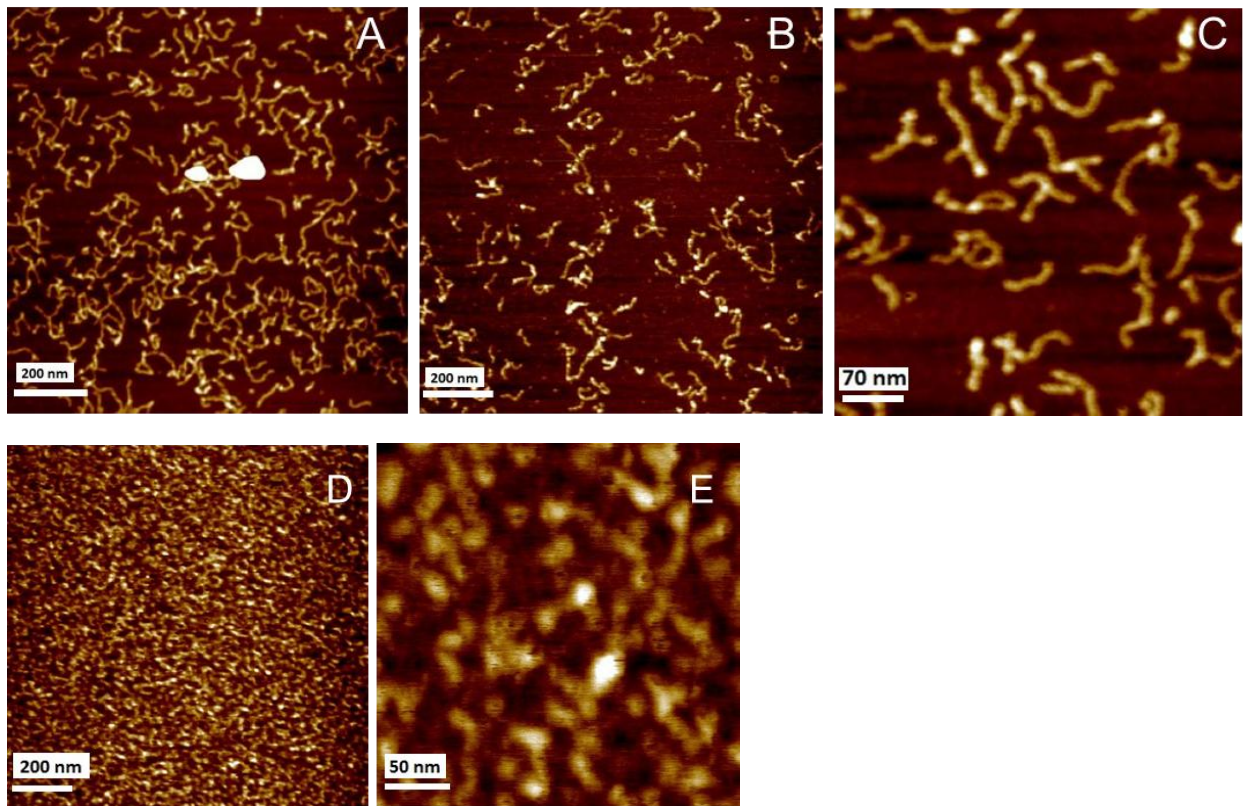


Figure S12. Typical AFM images of the studied complexes: M30/N30 (A, B, C), M30D/N30D (D, E).

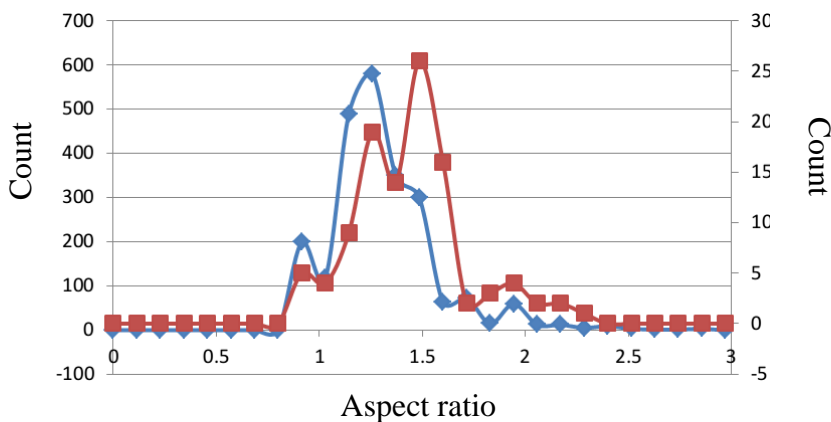


Figure S13. Aspect ratio of the complexes M20D/N20D (blue, left axis), M20D/N20DI/S10I (1:1:1, brown, right axis) obtained by AFM analysis.

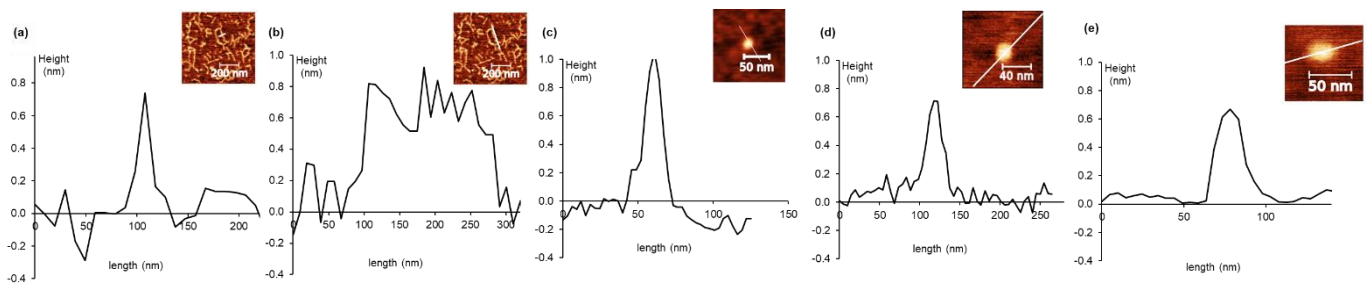


Figure S14. Height analysis of the AFM images of the complexes studied: (a), (b) M20/N20; (c) M20D/N20D; (d) M20D/N20DI; (e) M20D/N20DI/S10I.

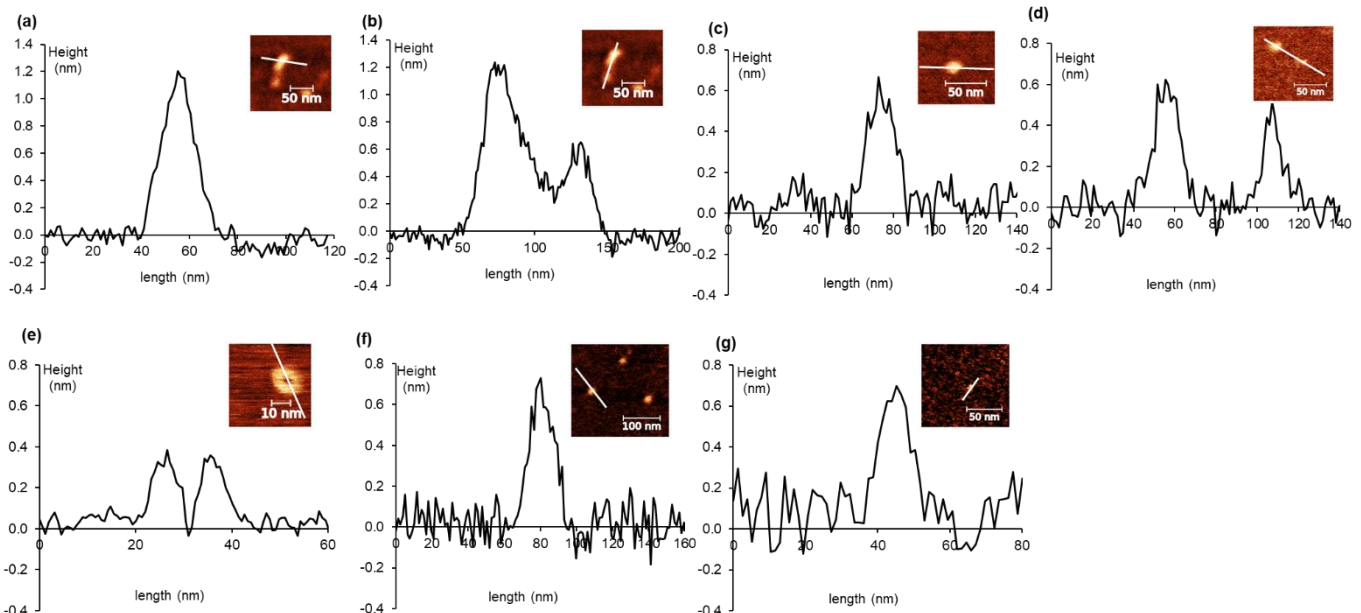


Figure S15. Height analysis of the AFM images of the complexes studied: (a), (b) M20T1/N20; (c) M20T5/N20T3; (d) M20T10/N20T5; (e) M20T25/N20T2; (f) M20T25/N20T5; (g) M20T25/N20T25.

Molecular dynamics simulation and analysis

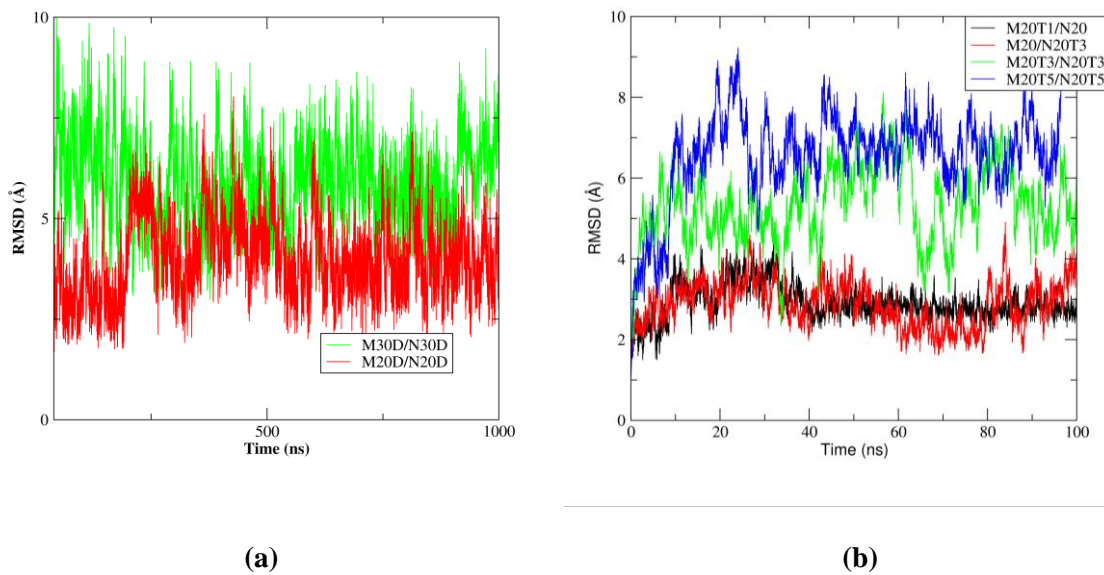


Figure S16. RMSD values along the MD trajectories for complexes with (a) non-nucleotide modifications and (b) native with different loop blocks.

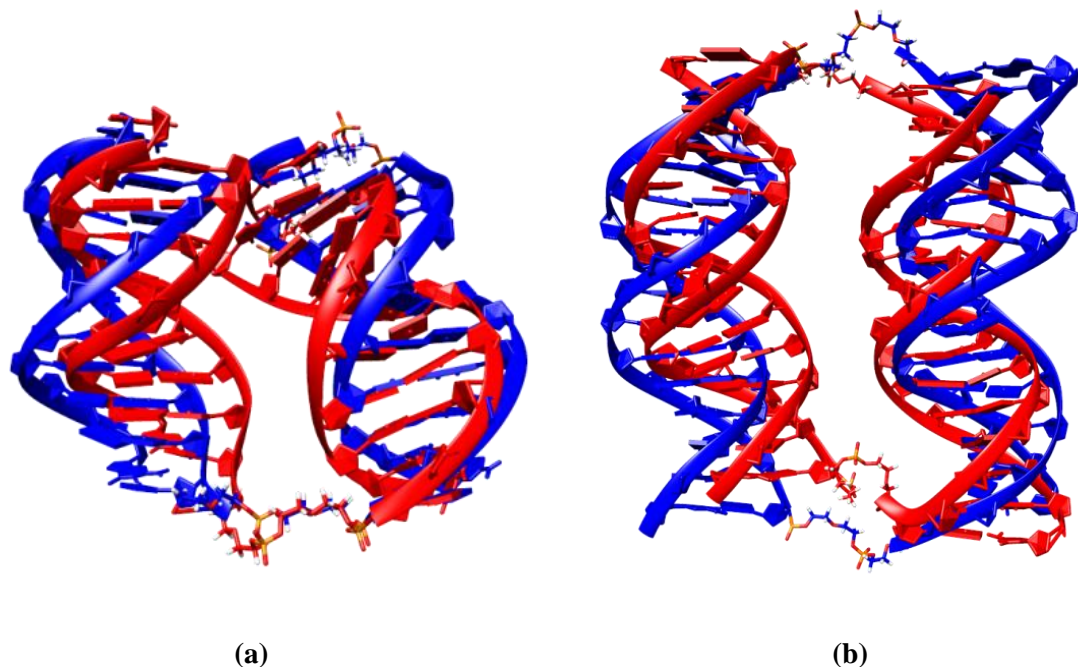


Figure S17. Comparison of the most representative structures in MD trajectories obtained by cluster analysis for complexes (a) M20D/N20D and (b) M30D/N30D in the presence of only Na⁺ ions (blue) and in mixture of Na⁺ and Mg²⁺ (red). Fifteen magnesium ions were added into simulation box.

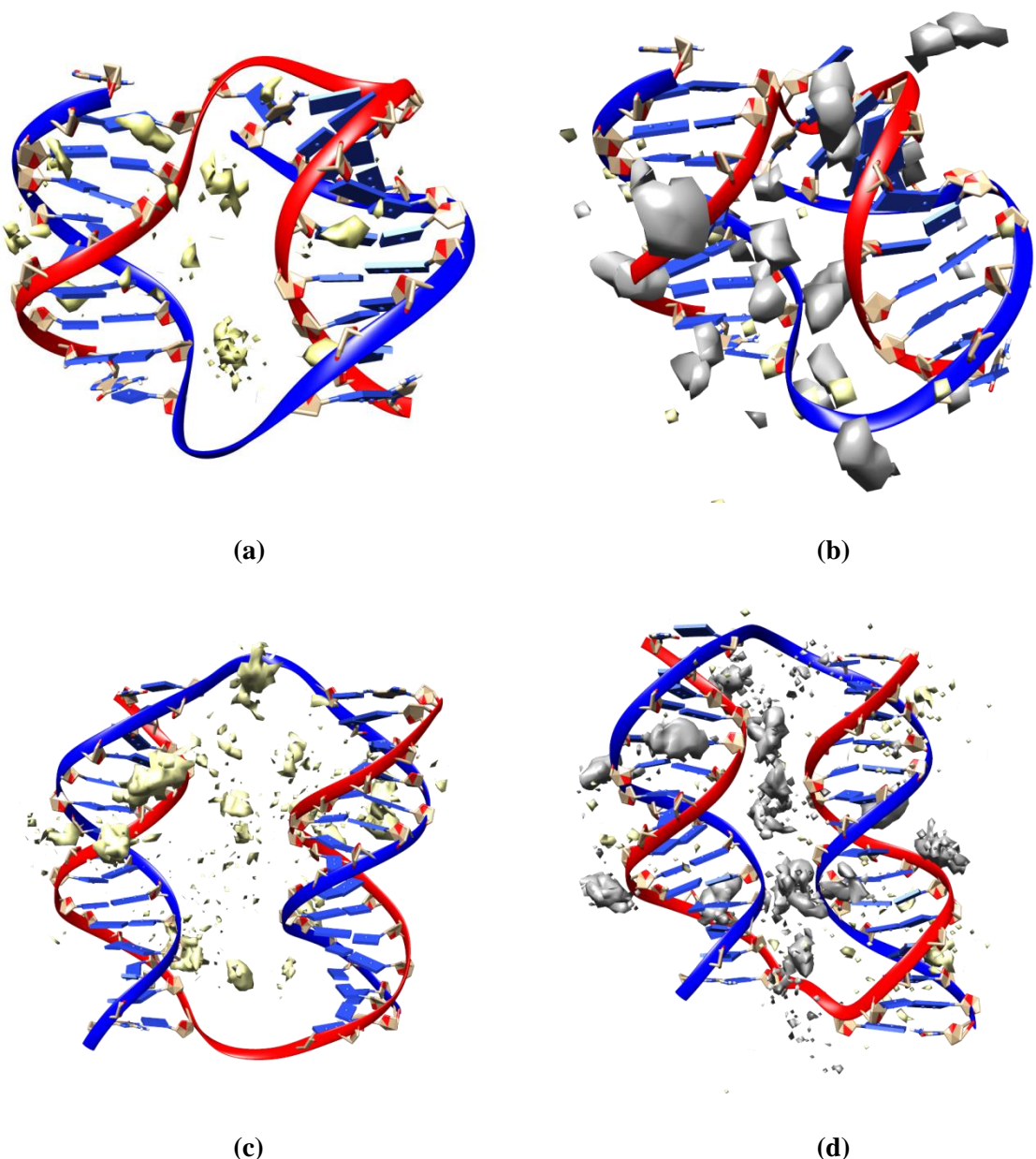


Figure S18. Comparison of the sodium (yellow) and magnesium (gray) density maps for complexes **(a,b)** M20D/N20D and **(c,d)** M30D/N30D in the presence of only Na^+ ions (a,c) and in mixture of Na^+ and Mg^{2+} **(b,d)**.

Table S4. Summary of cluster analysis of 100 ns MD simulation of studied complexes

| #Cluster | M20D/N20D | | | | M30D/N30D | | | |
|-------------|-----------|----------------------|-------|-----------------------|-----------|---------|-------|----------|
| | Frac | AvgDist ¹ | Stdev | AvgCDist ² | Frac | AvgDist | Stdev | AvgCDist |
| 0 | 0.712 | 4.318 | 1.002 | 6.462 | 0.366 | 4.342 | 0.904 | 6.212 |
| 1 | 0.188 | 4.132 | 0.954 | 7.487 | 0.311 | 4.701 | 1.094 | 7.472 |
| 2 | 0.075 | 3.176 | 0.756 | 6.177 | 0.289 | 4.454 | 0.967 | 6.622 |
| 3 | 0.018 | 4.074 | 0.979 | 7.721 | 0.027 | 3.698 | 0 | 7.047 |
| 4 | 0.008 | 4.485 | 1.183 | 6.675 | 0.007 | 0 | 0 | 8.445 |
| M20/N20T3 | | | | M20T3/N20T3 | | | | |
| #Cluster | Frac | AvgDist | Stdev | AvgCDist | Frac | AvgDist | Stdev | AvgCDist |
| 0 | 0.713 | 2.793 | 0.579 | 3.759 | 0.605 | 3.283 | 0.678 | 5.277 |
| 1 | 0.108 | 2.734 | 0.401 | 3.839 | 0.176 | 3.558 | 0.713 | 4.746 |
| 2 | 0.088 | 2.89 | 0.418 | 3.851 | 0.142 | 3.061 | 0.854 | 6.016 |
| 3 | 0.071 | 2.019 | 0 | 4.161 | 0.059 | 2.706 | 0.73 | 5.086 |
| 4 | 0.021 | 1.771 | 0 | 4.101 | 0.018 | 0 | 0 | 6.231 |
| M20T5/N20T5 | | | | M20T1/N20 | | | | |
| #Cluster | Frac | AvgDist | Stdev | AvgCDist | Frac | AvgDist | Stdev | AvgCDist |
| 0 | 0.766 | 4.052 | 0.969 | 5.982 | 0.619 | 2.053 | 0.347 | 3.112 |
| 1 | 0.077 | 3.386 | 0.583 | 7.112 | 0.165 | 2.437 | 0.448 | 3.415 |
| 2 | 0.069 | 0 | 0 | 7.691 | 0.089 | 2.598 | 0.408 | 3.406 |
| 3 | 0.057 | 2.655 | 0.54 | 7.346 | 0.083 | 2.177 | 0.162 | 3.312 |
| 4 | 0.031 | 0 | 0 | 6.113 | 0.045 | 1.831 | 0 | 3.142 |

#Cluster – Cluster number starting from 0 (0 is most populated)

Frac – size of cluster as fraction of total trajectory

AvgDist – average distance between points in the cluster

Stdev - standard deviation of points in the cluster

AvgCDist - average distance of this cluster to every other cluster